

# A combined millimeter wave and CO<sub>2</sub> interferometer on the C-2W Jet plasma<sup>a)</sup>

R. J. Smith<sup>b)</sup> and TAE Team<sup>c)</sup>

TAE Technologies, Inc., Foothill Ranch, California 92610, USA

A two wavelength tangentially viewing multi-chord interferometer has been built for the Jet plasma of the C-2W experiment at TAE Technologies. A novel 1 mm wavelength interferometer has been developed to be used simultaneously with a CO<sub>2</sub> laser interferometer to provide full coverage of the Jet plasma and the translating field-reversed configuration (FRC) plasma before merging. With CO<sub>2</sub> and millimetre wave sources the interferometer proposes to cover a combined dynamic range of line integrated density of more than 1000 although the CO<sub>2</sub> interferometer sub-system is not yet operational. Sited at the axial location of the mirror field of C-2W, the interferometer will play a pivotal role in assessing the FRC before merging and the operation of the inner and outer divertors and particle outflow. The performance of the millimeter wave interferometer and recent measurements are discussed.

## I. INTRODUCTION – C-2W DEVICE

The C-2W device generates a field reversed configuration (FRC) plasma in a 1.6 m diameter Inconel confinement vessel (CV) by forming and accelerating two FRCs in opposite directions to collide and merge in the CV. This program has been highly successful in forming and sustaining the FRC using neutral-beam injection (NBI)<sup>i</sup> on the previous C-2U device.<sup>ii</sup> The FRC is stabilized by biasing from distant electrodes and a large divertor structure has been implemented. On C-2W, an inner divertor has been added between the formation section and the CV. This allows a volume for flux expansion to stagnate the flow of particle outflow of the scrape-off-layer (SOL) and allow the electron temperature to increase. The goal of C-2W is to explore FRCs with high electron temperature, as high as 1 keV; additionally, the NBI power has been increased and the capability of raising external magnetic field in the CV from 0.1 to 0.3 Tesla is in place. Plasma pulse duration can be eventually extended up to 30 milliseconds on C-2W. In sequence, the C-2W device has a mirror field at the ends of the CV, an inner divertor, a formation stage, an outer divertor and end electrode plates with a plasma gun on axis and mirror symmetric with respect to the CV mid-plane. The Jet plasma is the outflow of particles through the X points of the FRC equilibrium<sup>iii</sup>. The Jet outflow is important on experiments with longer FRC lifetimes as the Jet plasma may dominate the loss of inventory and its significance is not yet known for C-2W plasmas. The Jet interferometer is located at the north mirror region where the CV necks down to a 0.7 m inner diameter.

<sup>a)</sup>Published as part of the Proceedings of the 22nd Topical Conference on High-Temperature Plasma Diagnostics (HTPD 2018) in San Diego, California, USA.

<sup>b)</sup>Electronic mail: [rsmith@tae.com](mailto:rsmith@tae.com)

<sup>c)</sup>TAE Team members are listed in Nucl. Fusion **57**, 116021 (2017).

Plasma interferometers measure the difference in optical path length of a path containing the plasma relative to a path outside the plasma. The technique is sensitive to movements (vibrations) which produce a relative displacement in the paths,  $\Delta l$ , as well as a relative change of index of refraction along the path through the plasma of length,  $L_p$ . The refractive index of the plasma relative to air (unity) is proportional to the local electron density,  $n_e$ <sup>iv</sup>. The difference in optical path length is given as a phase,

$$\phi(t) = 2.82 \times 10^{-15} \lambda \int_0^{L_p} n_e(t) ds + 2\pi \Delta l(t) / \lambda [\text{rad}] \quad (1)$$

where the laser wavelength  $\lambda$  represents a phase of  $2\pi$  radians. A two wavelength,  $\lambda_1$  and  $\lambda_2$ , interferometer can discriminate between phase due to the plasma and phase from relative displacements. The plasma's line-integrated density (LID) is a profile independent quantity given by,

$$\int_0^{L_p} n_e ds = \frac{(\phi_1/\lambda_2 - \phi_2/\lambda_1)}{2.82 \times 10^{-15} (\lambda_1/\lambda_2 - \lambda_2/\lambda_1)} \quad (2)$$

and the relative displacement  $\Delta l$ , is given by,

$$\Delta l = -\frac{(\lambda_2 \phi_1 - \lambda_1 \phi_2)}{2\pi} \cdot \frac{1}{(\lambda_1/\lambda_2 - \lambda_2/\lambda_1)} \quad (3)$$

This system combines two millimeter wave ( $\lambda_1 = 1$  mm) and three CO<sub>2</sub> ( $\lambda_2 = 10.6$   $\mu\text{m}$ ) interferometers over five chords. Since the millimeter wave and CO<sub>2</sub> interferometers are not implemented on the same chord, Eqs (2) and (3) do not strictly apply. However, for the two adjacent diameter sightlines with mixed interferometers, these relations should hold. The movements are expected to be largely the same for all interferometers. This can be checked with vacuum discharges. With  $\lambda_1/\lambda_2 = 95$  the two effects decouple with LID approximately the first term of Eq. (1) using  $\phi_1$  and  $\lambda_1$  and  $\Delta l$  the second term using  $\phi_2$  and  $\lambda_2$ . For large LID, the CO<sub>2</sub> system can contribute to the first term and will be relied on if the millimeter wave system is cutoff (peak  $n_e > 10^{21} \text{m}^{-3}$ ) as the FRC moves past but this is an exceedingly brief time in which  $\Delta l$  does not change and two wavelength interferometry is not needed.

The Jet interferometer represents a challenge in dealing with plasmas that span a wide range of LID but also an opportunity to provide key measurements on the FRC before merging, the establishment of the equilibrium and Jet outflow, and the interaction of the inner and outer divertors as well as biasing and the use of the end plasma gun. The Jet plasma density is not well known but must be substantially less than the bulk plasma density. The translating FRC, at velocities exceeding 300 km/s, is compressed in the magnetic mirror region enhancing its peak density and reducing its length (FRCs contract axially when compressed radially), although the translating FRC represents only half of the particle inventory of the merged FRC equilibrium in the CV. A compact source is needed for this region with enough sensitivity to quantify a Jet plasma of relevance and yet have a high cutoff density. A longer wavelength FIR source is rejected by the limited space and by constraints placed on a Gaussian beam given the 1.6" port diameters separated by 1 meter. A CO<sub>2</sub> interferometer system deployed on C-2U<sup>v,vi</sup> was shown to be appropriate for the FRC. A novel 300 GHz interferometer was implemented on C-2W, as shown in Fig. 1; the arrangement of chords is also shown.

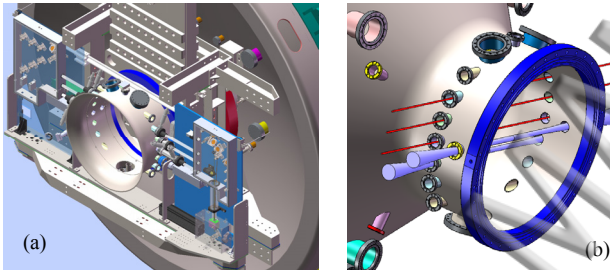


FIG. 1(a) The Jet interferometer layout showing the port array and gatevalve separating the CV from the inner divertor (b) the arrangement of CO<sub>2</sub> and mmwave probe beams. The CO<sub>2</sub> beams are pencil beams of about 6mm diameter, the millimeter beams are extended Gaussian beams with a 1.7 cm waist on the machine axis.

## II. DESCRIPTION OF THE INTERFEROMETER

### A. Mechanical support structure

Several considerations have dictated the design of the interferometer frame as shown in Fig. 2. The 2.5 m long

stainless steel optical table is supported by the C-2W frame but its width is limited to 0.2 m. The frame was designed as a stiff U shape with a garolite rod spanning the top to complete a rigid box structure. Stainless steel shear walls support the vertical panels off the optical table. The two panels are optical platforms for mirrors and beam splitters. The panel material is 0.5" thick phenolic, chosen to minimize phase distortion and beam misalignments due to the high magnetic fields in this region. These fields are static or changing on a slow time scale, and their effects should not be difficult to remove from the phase signals. The top of the panels is stabilized by three supports to the C-2W frame. Figure 2 shows the layout of the interferometer.

On the CV, the CO<sub>2</sub> system uses ZnSe viewports mounted on 2<sup>3</sup>/<sub>4</sub>" conflat flanges. The windows are anti-reflection (AR) coated. For the millimeter wave system, crystalline quartz windows mounted on a 3-3/8" conflat are used to provide the Gaussian beam with a generous aperture that matches the fundamental restriction of the 1.6" inner diameter of the ports. The quartz window aperture is a full 1.6" (Laser Optex Co.). The transmission through the quartz window can be significantly reduced by Fresnel reflection losses. Two windows were coated with an AR coating of parylene film (Tydex Co.). Parylene is a high vacuum compatible plastic, stable at high temperatures. Both surfaces of the window were coated yielding a transmission of 89%. The windows on the CV are at present uncoated but will be replaced.

The Gaussian beam of the millimeter wave sources has a diameter of 1.7" at the focusing lenses and the insertion loss of a window and its vacuum hardware was tested and found to be low.

There are 3 CO<sub>2</sub> probe beams and two independent millimeter wave interferometers and a 4<sup>th</sup> reference CO<sub>2</sub> interferometer independent of the plasma. Only for the two diameter chords, one mmwave and one CO<sub>2</sub> can vibrations and LID be separated but it is expected that the movements will apply to the two other CO<sub>2</sub> chords as well.

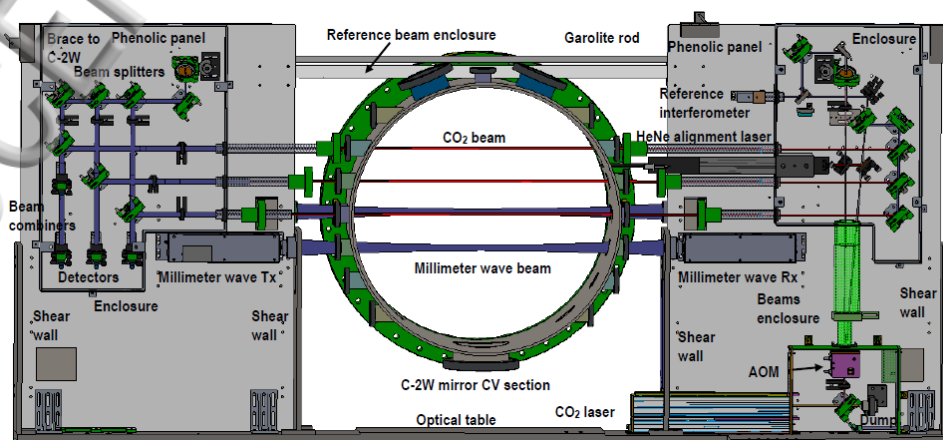


FIG. 2. Optical layout of Jet interferometer together with a section of the CV with array of ports to scale

## B. Millimeter wave interferometer

### a. Electronic scheme of the mmwave interferometer

The millimeter wave system is a heterodyne interferometer using two low noise 7.5 GHz dielectric resonant oscillators (DRO) and Impatt diodes as 40x multipliers to reach 300 GHz. A 2 MHz detuning of the receiving (Rx) DRO with respect to the fixed frequency of the transmitting (Tx) DRO produces a near 80 MHz RF IF out, as shown in Fig. 3 (Elva-1 Co.). The beat between the Tx and Rx sources is a sinusoidal RF output from the 2<sup>nd</sup> harmonic mixer. The output power is about 2 mW.

As originally intended, it was not possible to actively stabilize the RF IF 80 MHz beat which does drift as the

DRO sources drift with time. Therefore, a tracking signal (LO IF out) is provided to monitor this spurious phase excursion. The phase difference between the RF signal and the LO tracking signal determines the resolution of the interferometer, a 10° rms phase noise with 30 MHz bandwidth (BW) over 20 ms.

The millimeter wave output is coupled using an antenna coupler from fundamental waveguide to a free space Gaussian beam and focused to a waist on axis using HDPE lenses. The polarization is parallel to the external field (O-mode).

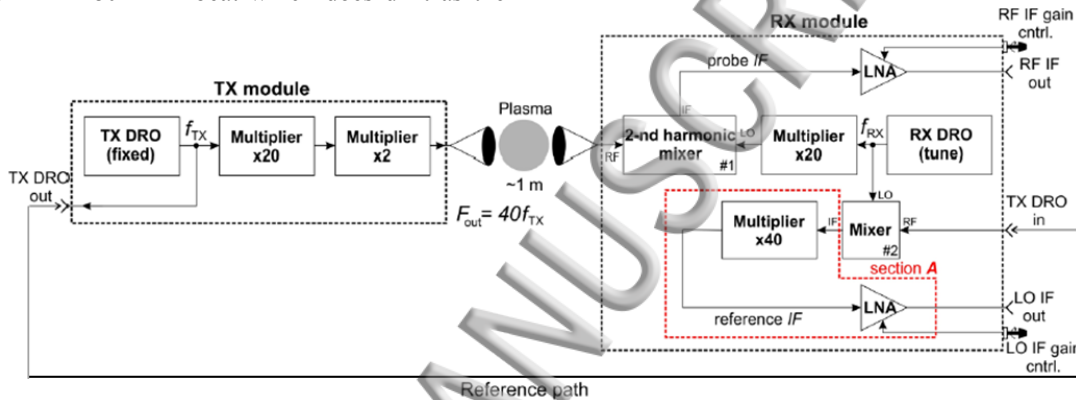


FIG. 3. Electrical schematic of the millimeter wave interferometer. (Elva-1 MMI-300R2)

### b. Demodulation of the plasma phase

The demodulation uses a ‘so-called’ running phase technique, which to this author’s knowledge has not been reported in the literature, in which phase traces are generated from the digitized RF signal and from a reference signal which may be the RF signal itself. The plasma trace is the difference of the two. This system required an LO tracking signal.

The phase noise floor for this method is determined by how steady the RF frequency is in time or how well the tracking signal tracks the RF phase. Heuristically, the RF 80 MHz beat is a phasor rotating at a measureable rate that is compared to a reference phasor rotating at a known rate. The accumulation of phase of one phasor relative to the other is the desired phase signal. As long as the relative rates between the phasors does not exceed 80 MHz, the phase is unambiguously determined. The running phase method eliminates the need of quadrature detection and the associated electronic equipment which may degrade the fidelity of the measurement. The method requires a high digitization rate of at least twice the highest spectral component in the signal to satisfy Nyquist theorem. For this system, the data is digitized at 250 MS/s. The highest frequency component is 110 MHz and the system bandwidth is 30 MHz.

The RF signal phase is given by,

$$\phi_{RF}(t) = (\phi_{Rx} - \phi_{Tx}) + \phi_{plasma}(t) + \phi_{\Delta}(t) + \phi_{spurious}(t) \quad (4)$$

where  $(\phi_{Rx} - \phi_{Tx})$  is a steady  $\sim 80\text{MHz} \cdot 2\pi t$  radians. The LO signal phase is given by,

$$\phi_{LO}(t) = (\phi_{Rx} - \phi_{Tx}) + \phi_{spurious}(t) \quad (5)$$

which is the interferometer phase signal without any contributions from the plasma. Subtracting  $\phi_{LO}(t)$  from  $\phi_{RF}(t)$  is the desired  $\phi_{plasma}(t) + \phi_{\Delta}(t)$ . The intrinsic, instantaneous phase noise of  $\sim 1^\circ$ , an LID of  $0.6 \times 10^{16} \text{ m}^2$  as shown in Fig. 4. The noise in the accumulated phase is  $\sim 10^\circ$  at any time in a 20-millisecond acquisition (Fig. 5).

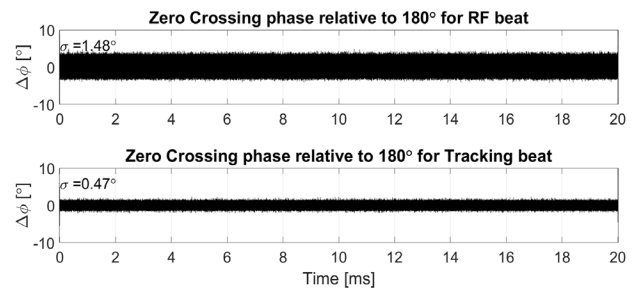


FIG. 4. Benchtop characterization of a mmwave system. The jitter in the time between zero crossings relative to the average half period for both RF and tracking signals in a 30 MHz bandwidth. The probe beam has more phase noise than the tracking signal.

One can do no better in determining the accumulated phase traces of the RF and LO signals than by measuring the timing of the signal’s zero crossings and assigning a phase of  $\pi$  per crossing. The rate of zero crossings is  $\sim 160$  per microsecond and over samples the phase traces. Accurately determining the time for each crossing is achieved by zero padding the signal in the frequency domain to generate more sampled points in the time domain and using 2-point linear interpolation. Zero

scattering factors of 5 and 10 did not change the result of Fig. 4, which shows the rms jitter in the half cycle duration is less than  $1.5^\circ$  relative to the average half cycle duration over 20 milliseconds.

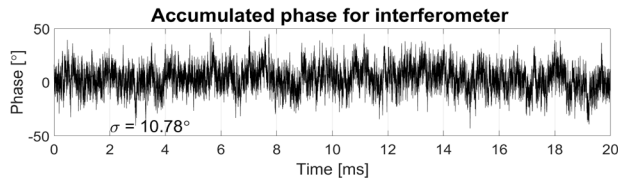


FIG. 5. The residual phase noise from differencing the accumulated phase from the RF and tracking signals.

The residual phase noise after the elimination of the spurious has an rms value of  $10^\circ$  and sets the phase noise floor, an equivalent LID of  $6 \times 10^{16} \text{ m}^{-2}$ .

### C. The CO<sub>2</sub> Interferometer

The CO<sub>2</sub> source is an RF excited laser (Synrad Co.) with an 11 W output polarized in the plane of the phenolic panel. About 1 W is split off to be divided between four CO<sub>2</sub> interferometers. The remaining 10 W is eliminated in a passively cooled beam dump. The laser is cooled to  $<20^\circ\text{C}$  for stable operation. The output is a Gaussian 3.5 mm diameter beam that expands to a 10 mm diameter at the detectors. Dichroic ZnSe beam splitters that pass 10.6  $\mu\text{m}$  and have a 50% reflection coefficient at 633 nm are used to allow a HeNe alignment laser to follow the CO<sub>2</sub> beams from source to detectors. All mirrors, detectors, and beam splitters lie in a plane with the exception of where the reference beam is shunted to the backside of the frame.

An acoustic optic modulator (AOM, Model #37040-5, Gouch & Housego Co.) splits the laser beam in two using a 35 W RF driver (Gouch & Housego Co.). The first order diffracted beam (scene beam) separates from the reference beam at an angle of  $4.7^\circ$ . The AOM imposes 40 MHz frequency offset on the diffracted beam. The undeflected reference beam is steered by mirrors to the back side and directed through a tube to reappear on the front side of the other panel in the optic plane. This displacement out of the optic plane is necessary to avoid the CV upper ports.

The optical components are fully contained in enclosures with interlocked covers to prevent accidental exposure to the beams. The laser output and power splitter are fully contained in an interlocked enclosure with re-entrant alignment posts to avoid exposure. Tubes connect enclosures.

About 92% of the angled scene beam is diverted to a series of two ZnSe 50/50 beam splitters and a mirror which direct the beams through the plasma at impact parameters of 0, 8.9 and 17.8 cm. The diameter chord is covered by both CO<sub>2</sub> and millimeter wave systems to provide a comparison of the two phase traces and a robust determination of  $\Delta l$  using Eq. (3). About 92% of the reference beam is steered to the other optical panel and similarly split into three beams using two beamsplitters and a mirror. The remaining 8% of the scene and reference beams is used for a 4<sup>th</sup> CO<sub>2</sub> interferometer completely contained within the panel enclosure to provide a measure of the phase noise originating from the AOM, a common mode contamination of all CO<sub>2</sub> interferometers.<sup>vi)</sup>

The scene and reference beams are combined onto the detectors using three ZnSe beam combiners. The detectors (Boston Electronic PVM10.6 HgCdTe photodiodes) are mounted in adjustable mounts that allow two axis tilt and translation to optimize the position of the detector. A 25.4 diameter ZnSe lens with a 25.4 mm focal length is used to focus the probe and reference beams onto the detectors.

The outputs are amplified and buffered for long coaxial cables to the quadrature mixers. A signal from the RF driver is used to down shift these signals to baseband producing sine and cosine signals which are digitized as detailed in Ref. 5. This system is essentially the same as the previous implementation

The CO<sub>2</sub> interferometer is complementary to the millimeter wave interferometer. The density of the translating FRC lies beyond the millimeter wave interferometer's range but is well characterize by the CO<sub>2</sub> system. This is important for quantifying the particle inventory and how successful the merging process of the FRCs retains this inventory. The millimeter wave system also gives a peak density fiducial of the translating FRC at cutoff which is a useful for profile information.

### D. Utility of the Jet interferometer

In addition to measuring the time trace of electron LID, the chords at four impact parameters will allow some useful density profile information if cylindrical symmetry can be invoked. Also, the bandwidths are very high, multi-MHz for the CO<sub>2</sub> system and 30 MHz for the millimeter wave system so that high frequency density fluctuations of low level can be observed.

C-2W experiments using the inner divertor, outer divertor, biasing and plasma gun should have dynamics that will be correlated with the Jet interferometer measurements. Determination of particle losses will be aided by the Jet interferometer and measurements of plasma flow.

## III. EXPERIMENTAL DATA

The CO<sub>2</sub> system is not yet operational and the millimeter wave interferometers were installed on C-2W to gain some experience. A problem with the strong magnetic field in the mirror region detuning the mmwave sources has been observed but not on all discharges. This has allowed both the FRC and Jet divertor LID to be quantified.

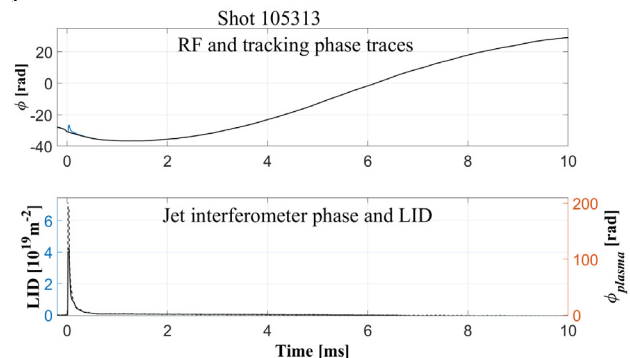


FIG. 6. Shot #105313, RF phase and tracking signal with the resultant phase upon differencing and LID.

Both the RF and tracking signal accumulated phases drift over many hundreds of degrees in 20 ms but the difference is small as shown in Figure 6.

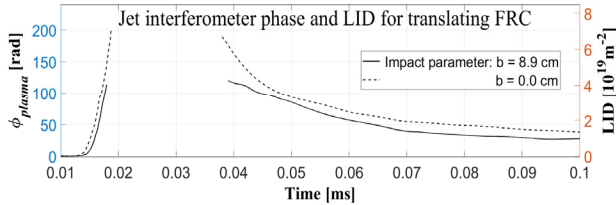


FIG. 7. Shot #105313, FRC phase and LID to cutoff. There is  $0.68 \mu\text{s}$  displacement of in leading edge of the FRC between the two systems.

Shot #105313 was without a mirror magnetic field and both millimeter wave interferometers produced data. The two interferometers are displaced axially by 9.54 cm which potentially provides an FRC translation velocity. Both systems entered cutoff, an electron density of  $1.1 \times 10^{21} \text{ m}^{-3}$  though Eq. (1) no longer applies near cutoff, the observation is significant and provides a peak density fiducial. A  $\text{CO}_2$  interferometer is 100 times less sensitive and appropriate for picking up the phase trace beyond cutoff. The FRC velocity is  $\sim 140 \text{ km/sec}$ , a lower bound, since the interferometers have different impact parameters and the plasma edge depends on this. The lower FRC profile is shorter. The final system will have both  $\text{CO}_2$  and millimeter wave interferometers on a diameter chord.

The two discharges illustrate the phase performance of the system with regards to bandwidth. A measured phase change of  $12,000^\circ$  in  $5 \mu\text{s}$  for the FRC is 7 MHz. The running phase signals must out run any foreseen phase slew rates. An RF beat of 80 MHz and BW of 30 MHz are appropriate. The 30MHz is set by the Nyquist frequency of the digitizer, 125 MHz, and the anti-aliasing filter which is 110 MHz. For more demanding implementations the frequencies can be doubled or tripled, an RF of 240 MHz, a bandwidth of 90 MHz and a 750 MS/s sampling rate or 375 MHz Nyquist frequency. This is the advantage of this technique.

Figure 8 shows a shot #105298 which reaches cutoff slightly after  $t = 0$  with LID of  $1.2 \times 10^{19} \text{ m}^{-2}$  as the FRC moves through the interferometer. A stable Jet plasma is established after a precursor density pulse with a stable period of 2.3 milliseconds and then decays away coincident with the termination of the FRC in the CV. The LID level correlates well with the CV mid-plane FIR chord LID at 5 ms when there is a uniform plasma density along the length of the vessel. The FRC's radius, 40 cm, is given by the excluded flux radius plot of Fig. 8. The vessel's radius at the Jet interferometer is 35 cm almost the same. So the LID in the Jet plasma is only 10 times lower than that of the FRC in the CV for this operational regime.

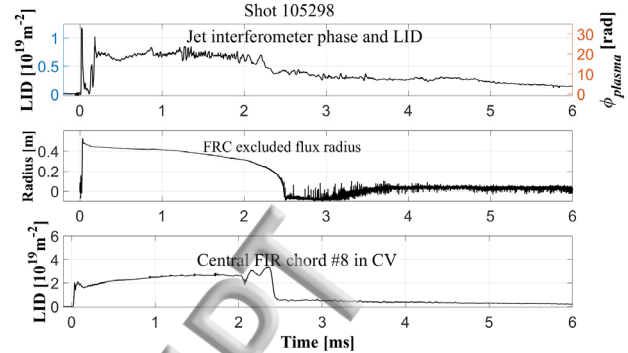


FIG. 8. Phase and LID for the Jet plasma together with the FRC's central LID and excluded-flux radius in the CV.

#### IV. SUMMARY

A two wavelength multi-chord tangentially viewing interferometer system has been designed and partially completed to diagnose the density distribution of the C-2W plasma at the axial location of the magnetic mirror. The millimeter wave interferometer system has measured the FRC LID up the  $10^{21} \text{ m}^{-3}$  cutoff and Jet plasma LID to be on the order of  $5 \times 10^{18} \text{ m}^{-2}$ . The Jet plasma is sufficiently tenuous to be diagnosed with a millimeter wave system. The observed Jet plasma LID is a phase of  $\sim 1000^\circ$  which this system can resolve to an accuracy of 1% or less. The FRC is over dense for the millimeter wave system confirming that a  $\text{CO}_2$  interferometer will provide complementary and complete measurements for full coverage of both FRC and Jet plasmas.

#### ACKNOWLEDGEMENTS

We thank our shareholders for their support and trust, and all fellow TAE staff for their dedication, excellent work, and extra efforts.

<sup>i</sup> Binderbauer M. M. *et al.*, "A high performance field-reversed configuration", *Phys of Plasmas*, **22** (2015), 056110

<sup>ii</sup> H. Gota *et al.*, "Achievement of Field-Reversed Configuration Plasma Sustainment via 10 MW Neutral-Beam Injection on the C-2U Device", *Nucl. Fusion* **57**, 116021 (2017).

<sup>iii</sup> M. Tuszewski, "Field Reversed Configurations", *Nuc. Fusion* **28**, (1988), p 2057

<sup>iv</sup> I. H. Hutchinson, *Principles of Plasma Diagnostics*, (Cambridge University Press, 2<sup>nd</sup> edition(2002).

<sup>v</sup> Gomostaeva O., Beng B. H., Garate E., Gota H., Kinley J., Schroeder J., Tuszewski M., (2010), "Two-color  $\text{CO}_2/\text{HeNe}$  laser Interferometer for C-2 experiment", *Rev. Sci. Instrum.*, **81**, 10D516.

<sup>vi</sup> Beall M., Deng G. H., Gota H., "Improved density profile measurements in the C-2U advanced beam-driven Field-Reversed Configuration (FRC) plasmas", *Rev. Sci. Instrum.*, **87**, 11E128.